CHAPTER FOUR

Gram-scale preparation of the antibiotic lead compound salicyl-AMS, a potent inhibitor of bacterial salicylate adenylation enzymes

Nihar Kinarivala[a], Lisa C. Standke[b], Tezcan Guney[a], Cheng Ji[a], Naoyoshi Noguchi[c,†], Yasutomi Asano[c,‡], Derek S. Tan[a,b,d,*]

[a]Chemical Biology Program, Sloan Kettering Institute, Memorial Sloan Kettering Cancer Center, New York, NY, United States
[b]Pharmacology Program, Weill Cornell Graduate School of Medical Sciences, Memorial Sloan Kettering Cancer Center, New York, NY, United States
[c]Tri-Institutional Therapeutics Discovery Institute, New York, NY, United States
[d]Tri-Institutional Research Program, Memorial Sloan Kettering Cancer Center, New York, NY, United States
*Corresponding author: e-mail address: tand@mskcc.org

Contents

† Present address: Research Division, Scohia Pharma, Inc., Shonan Health Innovation Park, 26-1, Muraoka-Higashi 2-chome, Fujisawa, Kanagawa 251-8555, Japan.
‡ Present address: Discovery Science, Axcelead Drug Discovery Partners, Inc., Shonan Health Innovation Park, 26-1, Muraoka-Higashi 2-chome, Fujisawa, Kanagawa 251-0012, Japan.

Methods in Enzymology, Volume 638
ISSN 0076-6879
https://doi.org/10.1016/bs.mie.2020.04.051

Abstract

Salicyl-AMS (**1**) is a potent inhibitor of salicylate adenylation enzymes used in bacterial siderophore biosynthesis and a promising lead compound for the treatment of tuberculosis. An optimized, multigram synthesis is presented, which provides salicyl-AMS as its sodium salt (**1**·**Na**) in three synthetic steps followed by a two-step salt formation process. The synthesis proceeds in 11.6% overall yield from commercially available adenosine 2′,3′-acetonide and provides highly purified material.

1. Introduction

Tuberculosis remains a global public health crisis, with an estimated 10 million new cases and 1.5 million deaths in 2018 (Furin, Cox, & Pai, 2019; World Health Organization, 2019). Current treatments are effective against drug-sensitive infections, but multi-drug resistant and extensively-drug resistant tuberculosis present major threats, and an estimated 484,000 new infections resistant to the first-line drug rifampicin were reported in 2018. Thus, there is a great need for new antibiotics to treat drug-resistant tuberculosis infections. *Mycobacterium tuberculosis*, the bacteria that causes tuberculosis, acquires the essential nutrient Fe^{3+} using iron-chelating molecules called siderophores (De Voss, Rutter, Schroeder, & Barry, 1999; De Voss, Rutter, Schroeder, Su, et al., 2000; Quadri & Ratledge, 2005; Ratledge, 2004). Siderophores bind iron with very high affinity and are used to transport iron across the cell envelope. Accordingly, inhibition of siderophore biosynthesis to limit bacterial iron uptake has been advanced as promising new antibacterial strategy (Lamb, 2015).

In collaboration with the laboratory of Luis Quadri, we have previously reported the development of the first designed siderophore biosynthesis inhibitor, salicyl-AMS (5′-*O*-[*N*-salicylsulfamoyl]adenosine) (**1**) (Fig. 1A) (Bythrow, Mohandas, Guney, Standke, et al., 2019; Ferreras, Ryu, Di Lello, Tan, et al., 2005). Salicyl-AMS is a potent inhibitor of MbtA, a salicylate adenylation enzyme that catalyzes the first step in the synthesis of the *M. tuberculosis* mycobactin siderophores **2** (McMahon, Rush, & Thomas, 2012; Quadri, Sello, Keating, Weinreb, et al., 1998). Salicyl-AMS mimics a tightly-bound reaction intermediate, salicyl-AMP (**4**), and potently inhibits MbtA biochemical activity as well as *M. tuberculosis* siderophore production and bacterial growth in cell culture. In collaboration with the laboratory of William Bishai, we demonstrated promising

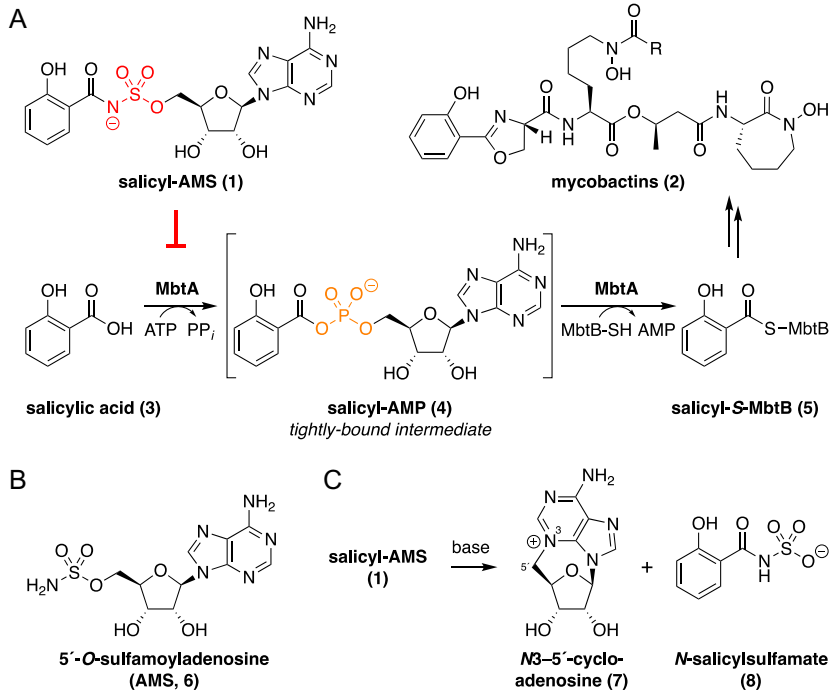

Fig. 1 (A) Salicyl-AMS (**1**) is a potent inhibitor of the salicylate adenylation enzyme MbtA, and mimics a tightly-bound salicyl-AMP intermediate (**4**), blocking production of the mycobactin siderophores (**2**). R represents various fatty acyl chains (mycobactin variants) or chains terminating in a carboxylate or methyl ester (carboxymycobactin variants). (B) Structure of highly toxic fragment 5′-*O*-sulfamoyladenosine (AMS, **6**). (C) Potential decomposition of salicyl-AMS (**1**) leading to *N*3–5′-cycloadenosine (**7**) and *N*-salicylsulfamate (**8**).

in vivo efficacy of salicyl-AMS in a mouse model of tuberculosis (Lun, Guo, Adamson, Cisar, et al., 2013). Aldrich and coworkers have also reported extensive structure–activity relationship studies of salicyl-AMS analogs (Dawadi, Boshoff, Park, Schnappinger, et al., 2018; Dawadi, Kawamura, Rubenstein, Remmel, et al., 2016; Dawadi, Viswanathan, Boshoff, Barry 3rd, et al., 2015; Duckworth, Nelson, & Aldrich, 2012; Engelhart & Aldrich, 2013; Gupte, Boshoff, Wilson, Neres, et al., 2008; Krajczyk, Zeidler, Januszczyk, Dawadi, et al., 2016; Nelson, Viswanathan, Dawadi, Duckworth, et al., 2015; Neres, Labello, Somu, Boshoff, et al., 2008; Qiao, Gupte, Boshoff, Wilson, et al., 2007; Qiao, Wilson, Bennett, & Aldrich, 2007; Somu, Boshoff, Qiao, Bennett, et al., 2006; Somu, Wilson, Bennett, Boshoff, et al., 2006; Vannada, Bennett, Wilson, Boshoff, et al., 2006).

To enable further preclinical evaluation of salicyl-AMS, we report herein an optimized, scalable protocol for synthesis, purification, and analysis of salicyl-AMS. Importantly, this protocol provides salicyl-AMS that is free of the des-salicyl fragment 5′-*O*-sulfamoyladenosine (AMS, **6**) (Fig. 1B) (<0.0006 mol%, below the lower limit of detection), which is known to be highly cytotoxic (NCI-60 mean $GI_{50} = 1.8$ nM; NSC133114) (Bloch & Coutsogeorgopoulos, 1971; Jaffe, McCormack, & Meymerian, 1970; Rengaraju, Narayanan, Ganju, Amin, et al., 1986), as well as an *N*3–5′-cycloadenosine byproduct (**7**), which forms under basic conditions via a precedented pathway (Fig. 1C) (Duckworth, Geders, Tiwari, Boshoff, et al., 2011; Shi, Tiwari, Wilson, Seiler, et al., 2013; Shuman, Robins, & Robins, 1969). Moreover, salicyl-AMS is highly acidic at the acylsulfamate moiety ($pK_a \approx 1.5$) (Cisar & Tan,unpublished results; Somu, Boshoff, et al., 2006), and Aldrich has reported previously that conversion to the triethylammonium salt (**1·Et$_3$N**) provides increased storage stability (Somu, Boshoff, et al., 2006). Our protocol affords salicyl-AMS as the corresponding sodium salt (**1·Na**), which is more commonly used in pharmaceutical formulations (Paulekuhn, Dressman, & Saal, 2007), to enable its use in preclinical and potentially clinical studies.

2. Synthesis of salicyl-AMS, sodium salt

Salicyl-AMS (**1**) was synthesized in three steps from commercially available adenosine 2′,3′-acetonide (**13**), in up to 10-g scale and an overall yield of 14.4% (Fig. 2). The route incorporates numerous improvements to our original route (Ferreras et al., 2005), based on subsequent reports from our group and Aldrich and coworkers. Notably, only a single protecting group manipulation is required. Sulfamoyl chloride (**10**) was prepared by treatment of commercially available chlorosulfonylisocyanate (**9**) with formic acid (Fig. 2A) (Appel & Berger, 1958; Brodsky & Du Bois, 2005; Heacock, Forsyth, Shiba, & Musier-Forsyth, 1996). Salicylic acid, *N*-hydroxysuccinimide ester (**12**) was prepared by activation of commercially available salicylic acid (**11**) with dicyclohexylcarbodiimide and coupling with *N*-hydroxysuccinimide (Van Brussel & Van Sumere, 1978) (Fig. 2B).

Adenosine acetonide **13** reacted with sulfamoyl chloride (**10**) selectively at the 5′-hydroxyl in *N*,*N*-dimethylacetamide (Cisar, Ferreras, Soni, Quadri, et al., 2007; Ferreras, Stirrett, Lu, Ryu, et al., 2008; Okada, Iwashita, & Koizumi, 2000) to form 5′-*O*-sulfamoyladenosine 2′,3′-acetonide (**14**) in 62.5% yield (Fig. 2C). Acylation with salicylic acid, *N*-hydroxysuccinimide ester (**12**) using cesium carbonate base in

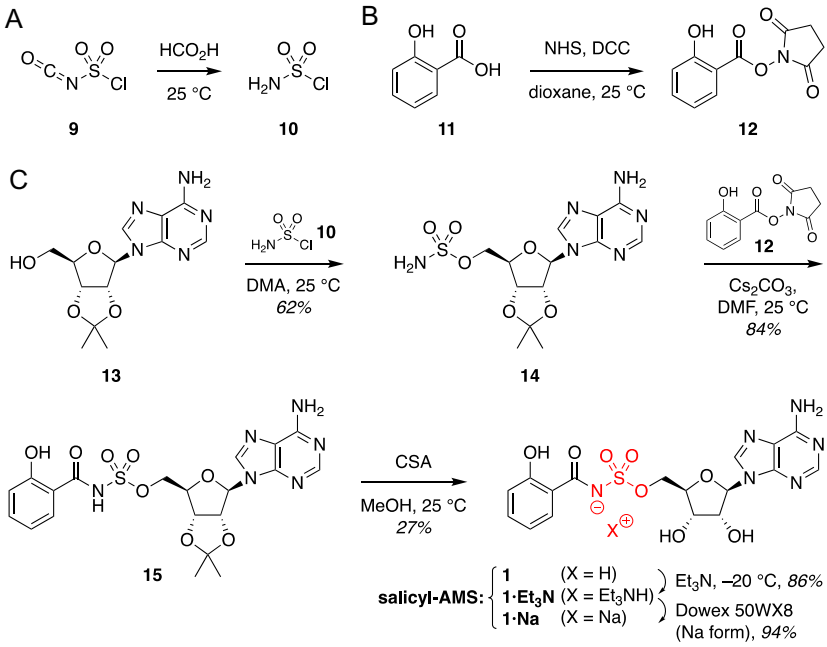

Fig. 2 (A) Preparation of sulfamoyl chloride (**10**). (B) Preparation of salicylic acid, *N*-hydroxysuccinimide ester (**12**). (C) Synthesis of salicyl-AMS (**1**) and conversion to the corresponding sodium salt (**1·Na**). CSA, camphorsulfonic acid; DCC, *N,N′*-dicyclohexylcarbodiimide; DMA, *N,N*-dimethylacetamide; DMF, *N,N*-dimethylformamide; NHS, *N*-hydroxysuccinimde.

N,N-dimethylformamide (Somu, Boshoff, et al., 2006) provided salicyl-AMS 2′,3′-acetonide (**15**) in 84.5% yield. Finally, deprotection was achieved most efficiently using camphorsulfonic acid in methanol to afford salicyl-AMS (**1**) in 27.3% yield (14.4% overall yield over three steps). This deprotection method provided higher yields compared to a variety of other conditions evaluated (5:2 trifluoroacetic acid [TFA]/H_2O; 3 equiv. TFA in 1:1 MeOH/H_2O; 3 equiv. toluenesulfonic acid in MeOH; 1 equiv. $BF_3{\cdot}Et_2O$ in CH_2Cl_2; 2 equiv. $FeCl_3$ in MeOH).

Salicyl-AMS was then converted to the corresponding sodium salt via a two-step procedure. Aldrich and coworkers have reported formation of the triethylammonium salt of salicyl-AMS directly from silica flash chromatography in the presence of 1% triethylamine (3:1 ethyl acetate/methanol) (Somu, Boshoff, et al., 2006). However, in our hands this led to incomplete conversion to the triethylammonium salt. Thus, we first attempted direct conversion of the free acid of salicyl-AMS (**1**) to the sodium salt **1·Na** using 1 equivalent of aqueous sodium hydroxide or 1 equivalent of

aqueous sodium bicarbonate at various temperatures (25 °C, 0 °C, −20 °C). However, all of these reactions resulted in formation of varying amounts of an *N*3–5′-cycloadenosine byproduct (**7**), which has been reported previously for related sulfamoyladenosines (Fig. 1C) (Duckworth et al., 2011; Shi et al., 2013; Shuman et al., 1969).

Accordingly, we turned to a two-step salt formation process involving initial conversion of salicyl-AMS to the stable, isolable triethylammonium salt, followed by salt exchange to the desired sodium salt. Thus, the free acid of salicyl-AMS (**1**) was treated with excess, freshly distilled triethylamine at −20 °C to form the triethylammonium salt **1·Et$_3$N**. Purification by silica flash chromatography (4:1 ethyl acetate/methanol with 1% Et_3N) removed the cycloadenosine byproduct **7** and afforded the triethylammonium salt of salicyl-AMS in 85.8% yield. Notably, increasing the reaction temperature from −20 °C to 0 °C or 25 °C resulted in increased formation of the cycloadenosine byproduct **7**.

Next, conversion of the triethylammonium salt **1·Et$_3$N** to the sodium salt **1·Na** was achieved using cation exchange on a Dowex 50WX8 column, which was washed rigorously with water, methanol, and acetonitrile, then pretreated with aqueous sodium hydroxide to generate the sodium form. A solution of salicyl-AMS, triethylammonium salt (**1·Et$_3$N**, 0.1 M) was passed through the column and the collected solution was lyophilized to provide the salicyl-AMS, sodium salt (**1·Na**) in 94.4% yield (81.0% overall yield from free acid, 11.6% overall yield from adenosine acetonide **13**). This salt formation protocol has been applied successfully to both small-scale (100 mg) and large-scale syntheses (2.5 g). Elemental analysis indicated a sulfur/sodium ratio of 1.43:1, comparable to the theoretical value of 1.39:1.

LC-MS/MS analysis of the salicyl-AMS free acid (**1**) indicated 0.31 mol % AMS as an impurity. In contrast, analysis of the final salicyl-AMS, sodium salt (**1·Na**) indicated <0.0006 mol% AMS, below the lower limit of detection. With appropriate minor modifications, this protocol has been applied to sodium salt formation with other salicyl-AMS analogs (Bythrow et al., 2019), and may also be useful for the preparation of acyl-AMS inhibitors of other targets in the adenylate-forming enzyme superfamily (Lux, Standke, & Tan, 2019).

2.1 Equipment

- Round bottom flask
- Stir bar
- Magnetic hot plate

- Septum
- Vacuum pump
- Vacuum/argon manifold
- Thermometer
- Sonicator (water bath)
- Chromatography columns (glass, various sizes)
- Distillation apparatus
- Rotary evaporator (Buchi)
- Lyophilizer
- Automated chromatography instrument (CombiFlash; Teledyn Isco)
- NMR spectrometer (400 or 500 MHz; Bruker)
- High-performance liquid chromatograph–mass spectrometer (LC-MS; Waters)
- High-performance liquid chromatograph–triple quadrupole mass spectrometer (LC-MS/MS; Agilent)

2.2 Chemicals

Reagents were obtained from Aldrich Chemical (www.sigma-aldrich.com), Acros Organics (www.fishersci.com), Alfa Aesar (www.alfa.com), or TCI America (www.tcichemicals.com) and used without further purification unless otherwise indicated. Optima or HPLC grade solvents were obtained from Fisher Scientific (www.fishersci.com), degassed with Ar, and purified on a solvent drying system unless otherwise indicated.

- Chlorosulfonylisocyanate
- Formic acid
- Petroleum ether
- Salicylic acid
- *N*-Hydroxysuccinimide
- 1,4-Dioxane
- *N*,*N*′-Dicyclohexylcarbodiimide
- *N*,*N*-Dimethylacetamide
- Sodium bicarbonate
- Sodium sulfate
- *N*,*N*-Dimethylformamide
- Cesium carbonate
- (1*S*)-(+)-10-Camphorsulfonic acid
- Triethylamine
- Dowex 50WX8 (hydrogen form)

- 1 N Sodium hydroxide solution
- Guanosine
- Methanol
- Ethyl acetate
- Water
- Acetonitrile
- Silica gel 60 thin-layer chromatography (TLC) plates with fluorescent indicator (F254)
- Silica gel 60 (230–400 mesh)
- Celite
- Phosphate buffered saline
- Dimethylsulfoxide

3. Protocol

All reactions were performed in flame-dried glassware under positive Ar pressure with magnetic stirring unless otherwise noted. Liquid reagents and solutions were transferred thru rubber septa via syringes flushed with Ar prior to use. Cold baths were generated as follows: 0 °C, wet ice/water; −25 °C, dry ice/acetone.

TLC was performed on 0.25 mm E. Merck silica gel 60 F254 plates and visualized under UV light (254 nm) or by staining with potassium permanganate ($KMnO_4$), or cerium ammonium molybdenate (CAM). Silica flash chromatography was performed manually on E. Merck 230–400 mesh silica gel 60 or on an ISCO CombiFlash Rf+ instrument with RediSep silica gel normal phase columns or RediSep Gold silica gel normal phase columns with UV detection at 254 nm.

NMR spectra were recorded on a Bruker UltraShield Plus 400MHz Avance III NMR or UltraShield Plus 600 MHz Avance III NMR with DCH CryoProbe at 24 °C in methanol-d_4 or DMSO-d_6.

3.1 Preparation of sulfamoyl chloride (10)

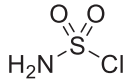

1. In a 100-mL round bottom flask, chlorosulfonylisocyanate (**9**) (20 g, 141.31 mmol, 12.27 mL, 1.0 equiv.) was cooled to 0 °C.
2. Formic acid (6.5 g, 141.31 mmol, 5.33 mL, 1.0 equiv.) was added dropwise to the reaction mixture at 0 °C.
3. The reaction mixture was allowed to warm to 25 °C and stirred for 1 h.

4. The reaction mixture was diluted with petroleum ether (50 mL), then filtered.
5. The filter cake was collected and dried under vacuum to give sulfamoyl chloride (**10**) (15 g) as a white solid, which was used without further purification.
6. *Note*: Chlorosulfonylisocyanate and sulfamoyl chloride are highly sensitive to moisture and react violently with water.

3.2 Preparation of salicylic acid, *N*-hydroxysuccinimide ester (12)

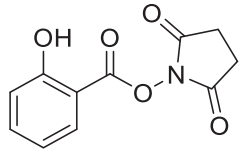

1. In a 2-L round bottom flask, salicylic acid (**11**) (42 g, 304.08 mmol, 1.0 equiv.) and *N*-hydroxysuccinimide (35 g, 304.08 mmol, 1.0 equiv.) were dissolved in 1,4-dioxane (700 mL) and cooled to 0 °C under nitrogen.
2. *N*,*N*′-Dicyclohexylcarbodiimide (62.74 g, 304.08 mmol, 61.51 mL, 1.0 equiv.) was dissolved in 1,4-dioxane (300 mL) and the solution was added to the reaction mixture.
3. The reaction mixture was allowed to warm to 25 °C and stirred for 12 h.
4. The reaction mixture was filtered to provide salicylic acid, *N*-hydroxysuccinimide ester (**12**) (76 g, crude) as a white solid, which was used without further purification.
5. ^{1}H NMR (DMSO-d_6, 400 MHz): δ 10.63 (br.s, 1H), 7.85 (dd, $J_1 =$ 1.6 Hz, $J_2 = 6.4$ Hz, 1H), 7.56 (td, $J_1 = 1.6$ Hz, $J_2 = 5.6$ Hz, 1H), 7.06 (d, $J = 8.4$ Hz, 1H), 6.98–6.96 (m, 1H), 2.87 (s, 4H).

3.3 Synthesis of 5′-*O*-sulfamoyladenosine 2′,3′-acetonide (14)

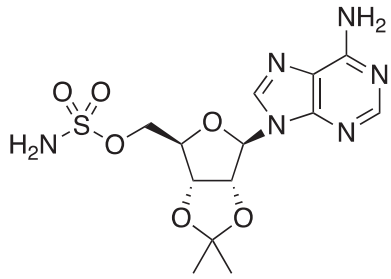

1. In a 1-L round bottom flask, adenosine 2′,3′-acetonide (**13**) (46 g, 149.69 mmol, 1.0 equiv.) was dissolved in *N*,*N*-dimethylacetamide (500 mL) and cooled to 0 °C under nitrogen.
2. Sulfamoyl chloride (**10**) (34.59 g, 299.38 mmol, 2.0 equiv., from Section 3.1) was added to the reaction mixture at 0 °C.
3. The reaction mixture was allowed to warm to 25 °C and stirred for 12 h with monitoring by LC-MS analysis of aliquots.
4. Upon completion, the reaction was quenched by addition of saturated aqueous sodium bicarbonate until the pH reached 7–8.
5. The mixture was extracted with ethyl acetate (5 × 500 mL), then the organic layers were combined, dried over sodium sulfate, filtered, and concentrated by rotary evaporation to provide a yellow residue.
6. The residue was purified by silica flash chromatography (ethyl acetate → 20:1 ethyl acetate/methanol) to afford 5′-*O*-sulfamoyladenosine 2′,3′-acetonide (**14**) (43 g, 84% purity: 93.48 mmol, 62.5% yield [adjusted for purity]) as a yellow oil.
7. LC-MS: $t_R = 1.092$ min, purity: 84%, m/z 387.0 $[M+H]^+$.
8. ^{1}H NMR (CD_3OD, 400 MHz): δ 8.27 (s, 1H), 8.22 (s, 1H), 6.25 (d, $J = 2.4$ Hz, 1H), 5.43 (dd, $J_1 = 2.0$ Hz, $J_2 = 6.0$ Hz, 1H), 5.14 (dd, $J_1 = 2.8$ Hz, $J_2 = 6.0$ Hz, 1H), 4.52–4.50 (m, 1H), 4.32–4.27 (m, 2H), 1.61 (s, 3H), 1.39 (s, 3H).

3.4 Synthesis of 5′-*O*-(*N*-salicylsulfamoyl)adenosine 2′,3′-acetonide (15)

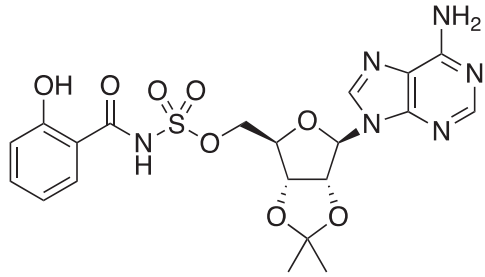

1. In a 1-L round bottom flask, 5′-*O*-sulfamoyladenosine 2′,3′-acetonide (**14**) (43 g, 84% purity: 93.48 mmol, 1.0 equiv. [adjusted for purity], from Section 3.3) was dissolved in *N*,*N*-dimethylformamide (450 mL) and cooled to 0 °C under nitrogen.

2. Salicylic acid, *N*-hydroxysuccinimide ester (**12**) (52.35 g, 222.58 mmol, 2.38 equiv., from Section 3.2) and cesium carbonate (108.78 g, 333.87 mmol, 3.57 equiv.) were added to the reaction mixture at 0 °C.
3. The reaction mixture was allowed to warm to 25 °C and stirred for 12 h with monitoring by LC-MS analysis of aliquots.
4. Upon completion, the reaction mixture was filtered and concentrated by rotary evaporation to provide a white residue.
5. The residue was purified by silica flash chromatography (1:1 petroleum ether/ethyl acetate → 20:1 ethyl acetate/methanol) to afford 5′-*O*-(*N*-salicylsulfamoyl)adenosine 2′,3′-acetonide (**15**) (40.2 g, 99.5% purity: 78.97 mmol, 84.5% yield [adjusted for purity]) as an off-white solid.
6. LC-MS: $t_R = 1.173$ min, purity: 99.5%, m/z 507.1 $[M+H]^+$.
7. ^{1}H NMR (CD_3OD, 400 MHz): δ 8.46 (s, 1H), 8.15 (s, 1H), 7.91 (dd, $J_1 = 1.6$ Hz, $J_2 = 7.6$ Hz, 1H), 7.33–7.29 (m, 1H), 6.82–6.79 (m, 2H), 6.25 (d, $J = 2.8$ Hz, 1H), 5.39 (dd, $J_1 = 2.8$ Hz, $J_2 = 6.0$ Hz, 1H), 5.16 (dd, $J_1 = 2.0$ Hz, $J_2 = 6.0$ Hz, 1H), 4.59–4.58 (m, 1H), 4.34 (dd, $J_1 = 2.8$ Hz, $J_2 = 4.0$ Hz, 2H), 1.60 (s, 3H), 1.27 (s, 3H).

3.5 Synthesis of salicyl-AMS (free acid) (1)

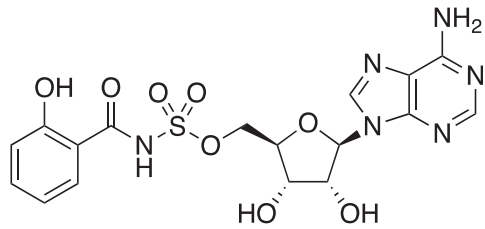

1. In a 1-L round bottom flask, 5′-*O*-(*N*-salicylsulfamoyl)adenosine 2′,3′-acetonide (**15**) (40.2 g, 99.5% purity: 78.97mmol, 1.0 equiv. [adjusted for purity], from Section 3.4) was dissolved in methanol (500 mL) and cooled to 0 °C under nitrogen.
2. Camphorsulfonic acid (55.04 g, 236.93 mmol, 3.0 equiv.) was added at 0 °C in one portion.
3. The reaction mixture was allowed to warm to 25 °C and stirred for 12 h with monitoring by LC-MS analysis of aliquots.
4. Upon completion, the reaction mixture was quenched by addition of solid sodium bicarbonate until the pH reached 7–8, then concentrated by rotary evaporation.

5. The residue was purified by silica gel chromatography (ethyl acetate → 5:1 ethyl acetate/methanol) to afford 25 g of partially purified product.
6. The partially purified product was further purified by preparative HPLC (column: Phenomenex Gemini C18 250 × 50 mm, 10 μm; mobile phase: water (0.05% v/v ammonia hydroxide) with 1–18% acetonitrile, 28 min). Lyophilization afforded salicyl-AMS (free acid) (**1**) (10.05 g, 99.9% purity: 21.53 mmol, 27.3% yield [adjusted for purity]) as a white solid.
7. ^{1}H NMR (CD_3OD, 400 MHz): δ 8.57 (s, 1H), 8.17 (s, 1H), 7.93 (dd, $J_1 = 1.6$ Hz, $J_2 = 8.0$ Hz, 1H), 7.29 (td, $J_1 = 1.6$ Hz, $J_2 = 7.2$ Hz, 1H), 6.80–6.75 (m, 2H), 6.09 (d, $J = 6.4$ Hz, 1H), 4.72 (t, $J = 5.6$ Hz, 1H), 4.42–4.40 (m, 2H), 4.37 (dd, $J_1 = 3.2$ Hz, $J_2 = 11.2$ Hz, 1H), 4.33–4.31 (m, 1H).

3.6 Conversion to triethylammonium salt (1·Et_3N)

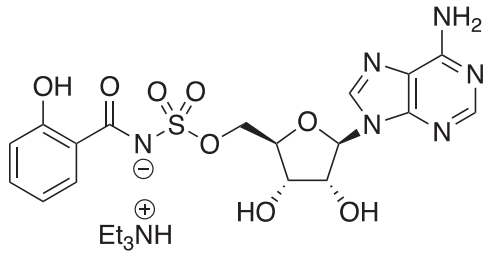

1. In a 250-mL round bottom flask, salicyl-AMS (free acid) (**1**) (2.5 g, 5.36 mmol, from Section 3.5) was dissolved in 200 mL methanol (27 mM).
2. The mixture was sonicated in a water bath for 5–10 min to increase solubilization.
3. The mixture was filtered using a 0.2 μM syringe filter.
4. The filtered solution was transferred to a 500-mL round bottom flask and cooled to −20 °C with stirring for 10 min.
5. *Note*: Salicyl-AMS may precipitate at temperatures below −25 °C.
6. Triethylamine (11.2 mL, 80.4 mmol, 15 equiv.) was added dropwise at −20 °C and the solution was stirred for 30 min at −20 °C.
7. *Note*: Freshly distilled triethylamine was used.
8. The reaction mixture was allowed to warm to room temperature and concentrated by rotary evaporation.

9. The residue was purified by silica flash chromatography (4:1 ethyl acetate/methanol + 1% triethylamine) to afford salicyl-AMS, triethylammonium salt (**1·Et$_3$N**) (2.61 g, 4.60 mmol, 85.8% yield) as a white solid.
10. *Note*: The crude product was dry-loaded onto the silica gel column by dissolving in 200 mL methanol, addition of 10 g Celite, rotary evaporation, and transfer of the Celite onto the column.
11. ^{1}H NMR (CD_3OD, 600 MHz): δ 8.41 (s, 1H), 8.13 (s, 1H), 7.94 (d, J = 7.8 Hz, 1H), 7.28 (t, J = 7.2 Hz, 1H), 6.72–6.87 (m, 2H), 6.08 (d, J = 6.4 Hz, 1H), 4.69 (t, J = 5.6 Hz, 1H), 4.24–4.34 (m, 4H), 3.17 (q, J = 7.2 Hz, 6H), 1.33 (t, J = 7.2 Hz, 9H) (Somu, Wilson, et al., 2006).

3.7 Conversion to sodium salt (1·Na)

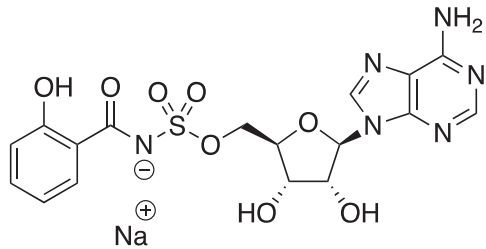

Table 1 Elemental analysis of salicyl-AMS, sodium salt (**1·Na**).

Sample	%C	%H	%N	%S	%Na
Experimental	38.65	3.89	15.54	6.39	4.47
Calculated	41.81	3.51	17.21	6.56	4.71

1. Dowex 50WX8 (hydrogen form) (1000 g) was placed in a glass column (3 in inside diameter × 12 in length, with 2000 mL reservoir).
2. The resin on the column was sequentially washed with water (5 × 1000 mL), methanol (5 × 1000 mL), water (5 × 1000 mL), acetonitrile (5 × 1000 mL), water (5 × 1000 mL) and 1 N aqueous sodium hydroxide (5 × 1000 mL).
3. The resin on the column was washed repeatedly with water until the eluent reached pH 7.

4. Salicyl-AMS, triethylammonium salt (**1·Et$_3$N**) (2.61 g, 4.60 mmol, from Section 3.6) was dissolved in minimal amount of 1:1 water/acetonitrile (≈50 mL).
5. The solution was loaded onto the Dowex column and incubated with the resin for 10 min.
6. The column was eluted with water (1000 mL) and 25-mL fractions were collected and analyzed by spotting on a TLC plate and visualizing under UV light (254 nm).
7. Fractions that were UV active were combined and lyophilized to afford salicyl-AMS, sodium salt (**1·Na**) (2.12 g, 4.34 mmol, 94.4% yield, 99.9% purity) as a fluffy white solid.
8. ^{1}H NMR (CD_3OD, 600 MHz): δ 8.55 (s, 1H), 8.19 (s, 1H), 7.97 (d, J = 7.6 Hz, 1H), 7.31 (t, J = 7.3 Hz, 1H), 8.70–6.84 (m, 2H), 6.12 (d, J = 6.4 Hz, 1H), 4.73 (t, J = 5.5 Hz, 1H), 4.34–4.44 (m, 4H).
9. Elemental analysis was performed to determine the percentage of carbon, hydrogen, nitrogen, sulfur, and sodium (Robertson Microlit). The sulfur:sodium ratio was calculated at 1.43:1, comparable to the theoretical ratio of 1.39:1 (1:1 molar ratio) (Table 1).

3.8 LC-MS/MS analysis of salicyl-AMS, sodium salt (1·Na) to quantify AMS impurity

3.8.1 Preparation of samples

1. Preparation of salicyl-AMS test sample solution: salicyl-AMS, sodium salt (**1·Na**) (2 mg) was dissolved in 0.4 mL of 9:1 phosphate buffered saline (PBS)/dimethylsulfoxide (DMSO) to generate a 5 mg/mL stock solution.
2. *Note*: The salicyl-AMS, sodium salt (**1·Na**) solution should be freshly prepared before use.
3. Preparation of guanosine internal standard solution: guanosine (2.5 mg) was dissolved in 0.5 mL DMSO to generate a 5 mg/mL stock solution. The stock solution was diluted 1000-fold with PBS to generate a 5 μg/mL working solution.
4. A calibration curve of AMS was prepared as follows:
   a. 5′-*O*-Sulfamoyladenosine (AMS, **6**) (Ferreras et al., 2005) (2 mg) was dissolved in 0.4 mL DMSO to generate a 5 mg/mL stock solution.
   b. The AMS stock solution was diluted 100-fold with PBS to generate a 50 μg/mL working solution.
   c. The 50 μg/mL AMS working solution was serially diluted twofold with PBS 12 times to generate calibration curve solutions at 50,

25, 12.5, 6.25, 3.13, 1.56, 0.781, 0.391, 0.195, 0.0977, 0.0488, 0.0244, 0.0122 μg/mL. A 0 μg/mL blank was also generated with PBS, for a total of 14 samples.

3.8.2 Preparation of 96-well plate

1. 100 μL of each salicyl-AMS calibration curve solution (from Section 3.8.1, step 4) was added to each well of 96-well plate, along with 100 μL of the internal standard working solution (from Section 3.8.1, step 3). The experiment was conducted in triplicates.
2. Final concentrations:
   a. Guanosine (internal standard): 2.5 μg/mL in all wells.
   b. AMS calibration curve: 0.061–25 μg/mL.
3. *Note*: When calculating the concentrations of the internal standard and of AMS in the samples, a dilution factor of 2 needs to be applied compared to the working solutions.

3.8.3 Method for LC-MS/MS analysis

LC-MS/MS analysis was carried out on an Agilent Technologies 6410 triple quadrupole LC-MS/MS system with autosampler in electrospray ionization (ESI) mode, with an Agilent Zorbax Eclipse XBD-C18 reverse phase column (50 × 4.6 mm, 5 μm) using a flow rate of 0.5 mL/min and an isocratic mobile phase of 10% acetonitrile in 0.1% aqueous formic acid over 10 min. Positive electrospray in multiple reaction monitoring (MRM) mode was employed to quantify AMS, using the ion transitions indicated below.

Compound	Precursor ion	Product ion	Fragmentor	Collision energy
AMS (**6**)	347.1	136.1	128	20
Guanosine	284.1	152.1	71	8

4. Concluding remarks

We have developed an efficient protocol for the multigram-scale preparation of the anti-tuberculosis lead compound salicyl-AMS as its sodium salt (**1**·**Na**). The process proceeds in three synthetic steps, followed by a two-step salt formation protocol, to afford the target compound in

11.6% overall yield from commercially available adenosine 2′,3′-acetonide (**13**). The two-step salt formation process includes an additional chromatographic purification and removes both a cycloadenosine byproduct (**7**) and a toxic trace impurity AMS (**6**), providing highly purified material suitable for preclinical evaluation. This protocol has been applied to milligram to multigram-scale syntheses, and with minor modifications to other salicyl-AMS analogs (Bythrow et al., 2019). We envision that this protocol may also be useful in the preparation of other acyl-AMS inhibitors of the adenylate-forming enzyme superfamily (Lux et al., 2019).

Acknowledgments

We thank Kazuyoshi Aso (Tri-Institutional Therapeutics Discovery Institute and Axcelead Drug Discovery Partners) and Makoto Fushimi (Tri-Institutional Therapeutics Discovery Institute and Takeda Pharmaceuticals) for helpful discussions and for coordinating large-scale synthesis of salicyl-AMS (free acid) at WuXi AppTec. Generous financial support was provided by the National Institutes of Health (R01 AI118224 to D.S.T.; F31 AI129244 and T32 GM073546-Gross to L.C.S.; and CCSG P30 CA008748 to C.B. Thompson) and the Tri-Institutional Therapeutics Discovery Institute.

Conflicts of interests

D.S.T. is an inventor on U.S. Patents 8,461,128 and 8,946,188, and D.S.T. and L.C.S. are inventors on U.S. Patent Application PCT/US2019/068107 based on this work.

References

Appel, R., & Berger, G. (1958). Hydrazinsulfonsäure-amide, I. Über das Hydrazodisulfamid. *Chemische Berichte*, *91*(6), 1339–1341.

Bloch, A., & Coutsogeorgopoulos, C. (1971). Inhibition of protein synthesis by 5′-sulfamoyladenosine. *Biochemistry*, *10*(24), 4395–4398. https://doi.org/10.1021/bi00800a007.

Brodsky, B. H., & Du Bois, J. (2005). Oxaziridine-mediated catalytic hydroxylation of unactivated 3° C-H bonds using hydrogen peroxide. *Journal of the American Chemical Society*, *127*(44), 15391–15393. https://doi.org/10.1021/ja055549i.

Bythrow, G. V., Mohandas, P., Guney, T., Standke, L. C., et al. (2019). Kinetic analyses of the siderophore biosynthesis inhibitor salicyl-AMS and analogues as MbtA inhibitors and antimycobacterial agents. *Biochemistry*, *58*(6), 833–847. https://doi.org/10.1021/acs.biochem.8b01153.

Cisar, J. S., Ferreras, J. A., Soni, R. K., Quadri, L. E. N., et al. (2007). Exploiting ligand conformation in the selective inhibition of non-ribosomal peptide synthetase amino acid adenylation with designed macrocyclic small molecules. *Journal of the American Chemical Society*, *129*, 7752–7753. https://doi.org/10.1021/ja0721521.

Cisar, J. S., & Tan, D. S., unpublished results.

Dawadi, S., Boshoff, H. I. M., Park, S. W., Schnappinger, D., et al. (2018). Conformationally constrained cinnolinone nucleoside analogues as siderophore biosynthesis inhibitors for tuberculosis. *ACS Medicinal Chemistry Letters*, *9*(4), 386–391. https://doi.org/10.1021/acsmedchemlett.8b00090.

Dawadi, S., Kawamura, S., Rubenstein, A., Remmel, R., et al. (2016). Synthesis and pharmacological evaluation of nucleoside prodrugs designed to target siderophore biosynthesis in *Mycobacterium tuberculosis*. *Bioorganic and Medicinal Chemistry*, *24*(6), 1314–1321. https://doi.org/10.1016/j.bmc.2016.02.002.

Dawadi, S., Viswanathan, K., Boshoff, H. I., Barry, C. E., 3rd, et al. (2015). Investigation and conformational analysis of fluorinated nucleoside antibiotics targeting siderophore biosynthesis. *Journal of Organic Chemistry*, *80*(10), 4835–4850. https://doi.org/10.1021/acs.joc.5b00550.

De Voss, J. J., Rutter, K., Schroeder, B. G., & Barry, C. E., 3rd (1999). Iron acquisition and metabolism by mycobacteria. *Journal of Bacteriology*, *181*(15), 4443–4451.

De Voss, J. J., Rutter, K., Schroeder, B. G., Su, H., et al. (2000). The salicylate-derived mycobactin siderophores of *Mycobacterium tuberculosis* are essential for growth in macrophages. *Proceedings of the National Academy of Sciences of the United States of America*, *97*(3), 1252–1257. https://doi.org/10.1073/pnas.97.3.1252.

Duckworth, B. P., Geders, T. W., Tiwari, D., Boshoff, H. I., et al. (2011). Bisubstrate adenylation inhibitors of biotin protein ligase from *Mycobacterium tuberculosis*. *Chemistry and Biology*, *18*(11), 1432–1441. https://doi.org/10.1016/j.chembiol.2011.08.013.

Duckworth, B. P., Nelson, K. M., & Aldrich, C. C. (2012). Adenylating enzymes in *Mycobacterium tuberculosis* as drug targets. *Current Topics in Medicinal Chemistry*, *12*(7), 766–796. https://doi.org/10.2174/156802612799984571.

Engelhart, C. A., & Aldrich, C. C. (2013). Synthesis of chromone, quinolone, and benzoxazinone sulfonamide nucleosides as conformationally constrained inhibitors of adenylating enzymes required for siderophore biosynthesis. *Journal of Organic Chemistry*, *78*(15), 7470–7481. https://doi.org/10.1021/jo400976f.

Ferreras, J. A., Ryu, J. S., Di Lello, F., Tan, D. S., et al. (2005). Small-molecule inhibition of siderophore biosynthesis in *Mycobacterium tuberculosis* and *Yersinia pestis*. *Nature Chemical Biology*, *1*(1), 29–32. https://doi.org/10.1038/nchembio706.

Ferreras, J. A., Stirrett, K. L., Lu, X., Ryu, J.-S., et al. (2008). Mycobacterial phenolic glycolipid virulence factor biosynthesis: Mechanism and small-molecule inhibition of polyketide chain initiation. *Chemistry and Biology*, *15*(1), 51–61. https://doi.org/10.1016/j.chembiol.2007.11.010.

Furin, J., Cox, H., & Pai, M. (2019). Tuberculosis. *Lancet*, *393*(10181), 1642–1656. https://doi.org/10.1016/S0140-6736(19)30308-3.

Gupte, A., Boshoff, H. I., Wilson, D. J., Neres, J., et al. (2008). Inhibition of siderophore biosynthesis by 2-triazole substituted analogues of 5′-*O*-[*N*-(salicyl)sulfamoyl]adenosine: Antibacterial nucleosides effective against *Mycobacterium tuberculosis*. *Journal of Medicinal Chemistry*, *51*(23), 7495–7507. https://doi.org/10.1021/jm8008037.

Heacock, D., Forsyth, C. J., Shiba, K., & Musier-Forsyth, K. (1996). Synthesis and aminoacyl-tRNA synthetase inhibitory activity of prolyl adenylate analogs. *Bioorganic Chemistry*, *24*(3), 273–289. https://doi.org/10.1006/bioo.1996.0025.

Jaffe, J. J., McCormack, J. J., & Meymerian, E. (1970). Trypanocidal properties of 5′-*O*-sulfamoyladenosine, a close structural analog of nucleocidin. *Experimental Parasitology*, *28*(3), 535–543. https://doi.org/10.1016/0014-4894(70)90121-9.

Krajczyk, A., Zeidler, J., Januszczyk, P., Dawadi, S., et al. (2016). 2-Aryl-8-aza-3-deazaadenosine analogues of 5′-*O*-[*N*-(salicyl)sulfamoyl]adenosine: Nucleoside antibiotics that block siderophore biosynthesis in *Mycobacterium tuberculosis*. *Bioorganic and Medicinal Chemistry*, *24*(14), 3133–3143. https://doi.org/10.1016/j.bmc.2016.05.037.

Lamb, A. L. (2015). Breaking a pathogen's iron will: Inhibiting siderophore production as an antimicrobial strategy. *Biochimica et Biophysica Acta*, *1854*(8), 1054–1070. https://doi.org/10.1016/j.bbapap.2015.05.001.

Lun, S., Guo, H., Adamson, J., Cisar, J. S., et al. (2013). Pharmacokinetic and *in vivo* efficacy studies of the mycobactin biosynthesis inhibitor salicyl-AMS in mice. *Antimicrobial Agents and Chemotherapy*, *57*(10), 5138–5140. https://doi.org/10.1128/aac.00918-13.

Lux, M. C., Standke, L. C., & Tan, D. S. (2019). Targeting adenylate-forming enzymes with designed sulfonyladenosine inhibitors. *Journal of Antibiotics (Tokyo)*, *72*(6), 325–349. https://doi.org/10.1038/s41429-019-0171-2.

McMahon, M. D., Rush, J. S., & Thomas, M. G. (2012). Analyses of MbtB, MbtE, and MbtF suggest revisions to the mycobactin biosynthesis pathway in *Mycobacterium tuberculosis*. *Journal of Bacteriology*, *194*(11), 2809–2818. https://doi.org/10.1128/JB.00088-12.

Nelson, K. M., Viswanathan, K., Dawadi, S., Duckworth, B. P., et al. (2015). Synthesis and pharmacokinetic evaluation of siderophore biosynthesis inhibitors for *Mycobacterium tuberculosis*. *Journal of Medicinal Chemistry*, *58*(14), 5459–5475. https://doi.org/10.1021/acs.jmedchem.5b00391.

Neres, J., Labello, N. P., Somu, R. V., Boshoff, H. I., et al. (2008). Inhibition of siderophore biosynthesis in *Mycobacterium tuberculosis* with nucleoside bisubstrate analogues: Structure–activity relationships of the nucleobase domain of 5′-*O*-[*N*-(salicyl)sulfamoyl]adenosine. *Journal of Medicinal Chemistry*, *51*(17), 5349–5370. https://doi.org/10.1021/jm800567v.

Okada, M., Iwashita, S., & Koizumi, N. (2000). Efficient general method for sulfamoylation of a hydroxyl group. *Tetrahedron Letters*, *41*(36), 7047–7051.

Paulekuhn, G. S., Dressman, J. B., & Saal, C. (2007). Trends in active pharmaceutical ingredient salt selection based on analysis of the Orange Book database. *Journal of Medicinal Chemistry*, *50*(26), 6665–6672. https://doi.org/10.1021/jm701032y.

Qiao, C., Gupte, A., Boshoff, H. I., Wilson, D. J., et al. (2007). 5′-*O*-[(*N*-acyl)sulfamoyl] adenosines as antitubercular agents that inhibit MbtA: An adenylation enzyme required for siderophore biosynthesis of the mycobactins. *Journal of Medicinal Chemistry*, *50*(24), 6080–6094. https://doi.org/10.1021/jm070905o.

Qiao, C., Wilson, D. J., Bennett, E. M., & Aldrich, C. C. (2007). A mechanism-based aryl carrier protein/thiolation domain affinity probe. *Journal of the American Chemical Society*, *129*(20), 6350–6351. https://doi.org/10.1021/ja069201e.

Quadri, L. E. N., & Ratledge, C. (2005). Iron metabolism in the tubercle bacillus and other mycobacteria. In S. T. Cole, K. D. Eisenach, & D. N. McMurrayet al. *Tuberculosis and the tubercle bacillus* (pp. 341–357). Washington, DC: ASM Press.

Quadri, L. E., Sello, J., Keating, T. A., Weinreb, P. H., et al. (1998). Identification of a *Mycobacterium tuberculosis* gene cluster encoding the biosynthetic enzymes for assembly of the virulence-conferring siderophore mycobactin. *Chemistry and Biology*, *5*(11), 631–645. https://doi.org/10.1016/s1074-5521(98)90291-5.

Ratledge, C. (2004). Iron, mycobacteria and tuberculosis. *Tuberculosis (Edinburgh)*, *84*(1–2), 110–130. https://doi.org/10.1016/j.tube.2003.08.012.

Rengaraju, S., Narayanan, S., Ganju, P., Amin, M., et al. (1986). 5′-*O*-Sulfamoyladenosine (defluoronucleocidin) from a *Streptomyces*. *Meiji Seika Kenkyu Nenpo*, *25*, 49–55.

Shi, C., Tiwari, D., Wilson, D. J., Seiler, C. L., et al. (2013). Bisubstrate inhibitors of biotin protein ligase in *Mycobacterium tuberculosis* resistant to cyclonucleoside formation. *ACS Medicinal Chemistry Letters*, *4*(12), 1213–1217. https://doi.org/10.1021/ml400328a.

Shuman, D., Robins, R. K., & Robins, M. J. (1969). The synthesis of adenine 5′-*O*-sulfamoyl nucleosides related to nucleocidin. *Journal of the American Chemical Society*, *91*(12), 3391–3392. https://doi.org/10.1021/ja01040a062.

Somu, R. V., Boshoff, H., Qiao, C., Bennett, E. M., et al. (2006). Rationally designed nucleoside antibiotics that inhibit siderophore biosynthesis of *Mycobacterium tuberculosis*. *Journal of Medicinal Chemistry*, *49*(1), 31–34. https://doi.org/10.1021/jm051060o.

Somu, R. V., Wilson, D. J., Bennett, E. M., Boshoff, H. I., et al. (2006). Antitubercular nucleosides that inhibit siderophore biosynthesis: SAR of the glycosyl domain. *Journal of Medicinal Chemistry*, *49*(26), 7623–7635. https://doi.org/10.1021/jm061068d.

Van Brussel, W., & Van Sumere, C. F. (1978). *N*-Acylamino acids and peptides. VI. A simple synthesis of *N*-acylglycines of the benzoyl and cinnamyl type. *Bulletin des Societes Chimiques Belges*, *87*(10), 791–797. https://doi.org/10.1002/bscb.19780871008.

Vannada, J., Bennett, E. M., Wilson, D. J., Boshoff, H. I., et al. (2006). Design, synthesis, and biological evaluation of beta-ketosulfonamide adenylation inhibitors as potential antitubercular agents. *Organic Letters*, *8*(21), 4707–4710. https://doi.org/10.1021/ol0617289.

World Health Organization. (2019). *Global tuberculosis report 2019*. https://www.who.int/tb/publications/global_report/en/.